Muons and Neutrons

Complementary Probes for Hydrogen in Metals

R. Hempelmann and D. Richter

Forschungszentrum Jülich, Germany

Experimental techniques using muons and neutrons as complementary probes yield unique information on diffusion and site occupancy in many types of metal/hydrogen systems, some of which are technologically important.

In particle physics it is the antiparticle of a heavy lepton, lying beyond the four elementary particles of everyday physics (u, d, e$^-$, ν). But in condensed matter it behaves like real matter, or more precisely, like a very light hydrogen isotope. It is called the positive muon μ$^+$. With one-ninth of the proton mass, the muon expands considerably the isotope range of the element with atomic number one. Quantum transport effects are made more pronounced owing to a small mass, so it has boosted diffusion research on light interstitials in metals. But the muon has also successfully played a passive role in metals as a local probe (radioactive tracer) to study the static and dynamic properties of concentrated metal hybrides. We shall use three examples to describe the merits and limitations of the muon spin rotation method as compared to the now so-called classical procedures of neutron scattering.

The Experimental Techniques [1, 2]
Neutrons

The most familiar neutron scattering technique is *coherent elastic* neutron scattering — neutron diffraction for short. The neutron partial waves originating from the different scattering centres interfere to give sharp scattering maxima at certain scattering angles (Bragg peaks), and the complete structure of the system under investigation

Rolf Hempelmann has worked at the Institute of Solid State Research, KFA Jülich, W-5170 Jülich, Germany since 1980. He received a Ph.D. from the Institute for Physical Chemistry, University of Münster, in 1976, where he then worked for four years.

Dieter Richter was appointed Director of the Institute of Solid State Physics, KFA Jülich, in 1989 and holds the chair of physical chemistry at the University of Münster. He studied at the TU Braunschweig and worked at KFA Jülich before receiving his Ph.D. from the RTWH Aachen in 1977. After a year at BNL, USA, he returned to Aachen for several years before becoming a senior scientist at the ILL, Grenoble.

can be unravelled from the diffractogram. In addition, *diffuse coherent* neutron scattering (coherent *Zwischenreflex* scattering) delivers information about lattice defects and short-range order, where a necessary condition is that the atoms under investigation scatter neutrons coherently (*i.e.* the coherent neutron scattering cross section is appreciable). Of the hydrogen isotopes, deuterium fulfills this condition so the structure of ordered metal hybrides has been determined using deuterated samples.

The diffuse coherent scattering procedure, however, does not work satisfactorily in systems with reduced or missing translational symmetry such as amorphous hydrides because interference is partially effective. A different method based on *incoherent inelastic* scattering, called neutron vibrational spectroscopy, can be applied to determine hydrogen sites if hydrogen interactions are negligible. The vibrational excitation energies of hydrogen in the potential minima at the interstitial sites are determined as these excitations are characteristic of each type of site. The incoherent scattering cross section enters the scattering function, so these investigations are performed on light hydrogen in metals exploiting the huge incoherent scattering cross section of hydrogen.

Incoherent neutron scattering is also used to investigate single particle diffusion. As the energy transfers involved are very small, this technique is called (incoherent) *quasielastic* neutron scattering. Here, the neutron partial wave originating from one hydrogen atom cannot interfere with that from another hydrogen atom. Interference with itself occurs, however, when a hydrogen atom performs diffusional jumps during the passage of a neutron wave packet: the leading part of the wave packet interferes with the trailing part, and the spatio-temporal development of the diffusion process can be derived from the interference pattern.

Muons

Methods dedicated to the investigation of muons in condensed matter go by the acronym μSR which stands for muon spin rotation/relaxation/resonance. Muons are generated by accelerating protons to about 500 MeV and directing them against low atomic number materials (graphite or beryllium): pions, the primary reaction products, decay with parity violation so that their decay products, the muons, are spin-polarized. These muons are implanted into the sample and after a lifetime of 2.2 μs they decay to a neutrino, an anti-neutrino and a positron. This decay also proceeds with parity violation and the positron is strongly emitted in the direction in which the spin of the muon happened to be pointing at the instant of its decay.

The decay of the muon, being an elementary process, is of course independent of the chemical environment of the muon. But prior to the decay, the muon spin couples to nuclear spins in the sample. The direction of the muon spin at the instant of decay (as recorded in μSR) methods) therefore contains information about the chemical state and the dynamics of the muon during its short life.

Muons are unique probes because they can be implanted into every metal, whereas hydrogen does not dissolve in most metals at low temperature (the exceptions are hcp metals like Y and Sc) but instead precipitates as ordered hydride phases. They occupy the same interstitial sites as hydrogen and, as in neutron scattering, lead to structural and diffusional information about metal/hydrogen systems. Apart from the absence of an external magnetic field for polarizing spins (muons enter as a polarized beam), the muon spin rotation method is reminiscent of the well known nuclear magnetic resonance NMR-T_2 (spin-lattice relaxation) technique, whereas muon spin relaxation is by the same token analogous to NMR-T_1 (spin-spin relaxation).

Quantum Diffusion [3–5]

The low temperature diffusion of muons has been mostly studied in aluminium and copper. Owing to the large nuclear moments of ^{27}Al, ^{63}Cu and ^{65}Cu, large depolarization effects take place if the muons move sufficiently slowly. Furthermore, impurities can be removed from these fcc metals down to the ppm range, whereas such a purity is not feasible for bcc metals. Magnetic substances like iron are also suitable (muon spin depolarization arises from the electronic moments of the host lattice).
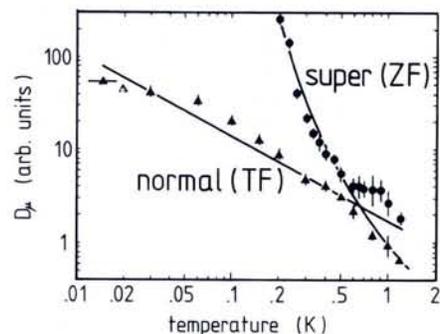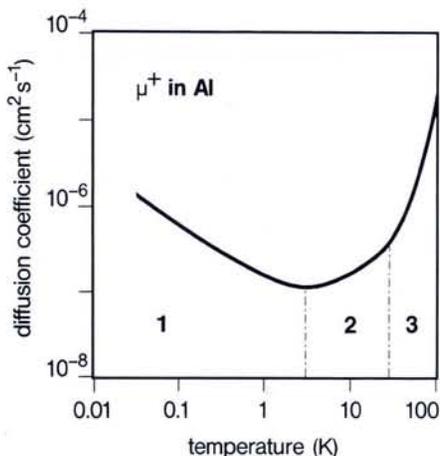
In practice, muon diffusion in pure Al is so fast that the regime of motional narrowing, where local spin fluctuations are averaged out by the motion of a muon, extends down to the millikelvin range, and the muon diffusion coefficient D can only be determined indirectly by studying diffusion-limited trapping of muons at impurities. A quantitative data evaluation along these lines in terms of a two-state model resulted in the temperature dependence of D displayed in Fig. 1: D exhibits a minimum at about 3 K and, remarkably, then *increases* with a decreasing temperature. At higher temperatures, D first passes through a regime with a linear T dependence and then goes over into a phonon-assisted tunnelling regime with an Arrhenius-like dependence.

The linear T dependence can be explained by processes in which only one phonon in the lattice is involved. These are forbidden in ideal lattices because of energy conservation, but are possible in the presence of lattice distortions, or for transitions between non-equivalent sites.

Electron scattering

The gradient of the muon diffusion coefficient at low temperatures is proportional to $T^{-0.7}$, in striking contrast to theory for phonon-assisted tunnelling which claims a T^{-9} behaviour for the transport of small polarons. This discrepancy between experiment and theory lasted for several years until suddenly at the end of 1984, J. Kondo [3] could impressively confirm the assumption, expressed several times, that electrons are involved in the low temperature diffusion mechanism. The principle feature is scattering of electrons at small polarons, leading to the correct T^{-1} dependence of D. However, the absolute value of the diffusion coefficient was several orders of magnitude too large.

A second and much more important effect of the muon-electron interaction consists in an additional temperature-dependent reduction of J_{eff}, the low-

Fig. 1 — A trapping model can be used to extract the diffusion coefficient of μ^+ in pure Al from the μ^+ depolarization rate. An estimate of the trapping radius is necessary. Three temperature regimes are recognizable: (3) Diffusion is supported by the interactions of the μ^+ with many lattice vibrations; the jump rate decreases with decreasing temperature. (2) One-phonon processes dominate. (1) With decreasing temperature, the diffusion coefficient or jump rate increases. The behaviour is mainly determined by the relaxation of the shielding electron cloud during the jump process. The smaller the temperature, the less pronounced is the influence of this relaxation on the tunnelling process. This means that at high temperatures the thermal movements support diffusion, whereas they prohibit it at low temperatures by disturbing the tunnelling processes between neighbouring sites.

Fig. 2 — The muon diffusion coefficient as a function of temperature in superconducting (ZF — zero field measurement) and normal (TF — transverse field measurement) states of Al with 75 ppm Li. Superconducting electrons (Cooper pairs) do not restrict muon diffusion.

temperature tunnelling matrix element. J_{eff} consists of a) the matrix element J_0 for tunnelling of bare muons (with no lattice distortion); b) a factor e^{-2S} which takes into account transport of the elastic shielding cloud (the small polaron) as the local distortion must also tunnel; c) an electronic factor — the new feature — such that

$$J_{eff}^2 = J_0^2\, e^{-2S} (kT/E_F)^{2K} \qquad (1)$$

where K is the muon-electron coupling parameter and E_F is the Fermi energy.

The muon has a positive charge and is shielded by an electron cloud assembled by the positive interference of electrons in appropriate Bloch states. The charge density of the conduction electron gas is primarily homogeneous in the ground state, i.e. at very low temperatures, so electrons have to be excited into states above the Fermi energy in order to shield the muon charge. This electron-hole excitation increases the kinetic energy, but the shielding cloud decreases the Coulomb energy; for the total system, the shielded state is energetically more favourable.

Effect on muon diffusion

The shielding cloud has to be dismantled at the old site and reassembled at the new site when the shielded muon

moves in a diffusional step to an adjacent site. At very low temperatures, where there are only very few electrons above the Fermi edge, there is hardly any overlap of the wave functions forming the old and new shielding clouds ("orthogonality catastrophe") and the electrons can no longer follow the movements of the muon adiabatically: the Born-Oppenheimer approximation, otherwise valid everywhere in solid-state and molecular physics, breaks down. From Eq. 1 and the golden rule we find at very low temperatures for electron-restricted tunnelling:

$$D \sim T^{2K-1} \qquad (2)$$

Calculated values of K obtained by estimating the scattering of an electron on the charged muon agree with experimental results, as do calculated values of D. In the high temperature range (phonon-assisted tunnelling, $T \geq 20$ K), the additional muon-electron coupling is of minor importance.

Direct experimental proof of the restricting effect of conduction electrons on muon diffusion at low temperatures was recently obtained in μSR measurements on μ^+ in normally conducting Al (in a transverse magnetic field larger than the upper critical field for superconductivity) and in superconducting Al (at zero field). Fig. 2 shows the results:

in the superconducting state, where electrons exist as Cooper pairs, electron scattering processes do not occur and the μ^+ diffusion coefficient increases strongly with decreasing temperature.

Hydrogen Diffusion in Hydrides [6, 7]
QNS
1. Experimental results

The classical method for unravelling the mechanism of hydrogen diffusion in metals is quasielastic neutron scattering (QNS). It is very well established for dilute solutions of hydrogen in metals, but is less so for ordered metal hydrides for mainly two reasons: a) single crystals are unavailable: QNS cannot be fully exploited with poly- or multidomaincrystals since much of the information which could in principle be obtained is blurred by averaging effects; b) only a small fraction of hydrogen atoms on antistructural sites is diffusionally active so a bulk technique such as, e.g., QNS or NMR, which sees all hydrogen atoms may not detect the active ones.

These difficulties were overcome recently in a QNS study of the ordered hydride β-VH$_{0.50}$. Large single domain crystals were grown in which hydrogen atoms occupy sets of octahedral sites, with nearly tetragonal point symmetry. Occupied layers (regular sites) therefore alternate with empty layers (antistructural sites). Sites in the latter begin to become occupied on increasing the temperature and, at 448 K, an order-disorder transition occurs involving the randomization of the H atoms over the two types of layers (an appreciable number of H atoms occupy antistructural sites just below this temperature).

The corresponding QNS spectra consist of narrow and broad quasielastic components: the former belong to fast diffusive jumps in the empty planes whereas the latter are due either to slow jumps, either in-plane in the occupied layers or out-of-plane. Thanks to the single crystal, the directional dependence of the QNS spectra allowed the two slow jumps to be distinguished (their linewidths are plotted in Fig. 3).

2. Analysis

A jump model (extended Chudley–Elliott) gave the following picture of the hydrogen diffusion mechanism. Consider a hydrogen atom originating in a filled layer: the probability of a jump into the empty layer is 3 to 6 times higher than for a jump among the occupied sites. Once the atom has moved into the empty layer, it performs 5 to 8 jumps before it drops into a vacancy in one of the two adjacent filled layers. Diffusion parallel to the sheets thus consists of

Fig. 3 — Quasielastic neutron scattering linewidths as a function of the reciprocal lattice vector Q for the slow diffusive motions of hydrogen in β-VH$_{0.50}$ as obtained from fits to different spectra. The solid lines represent the prediction of the extended Chudley-Elliot jump diffusion model.
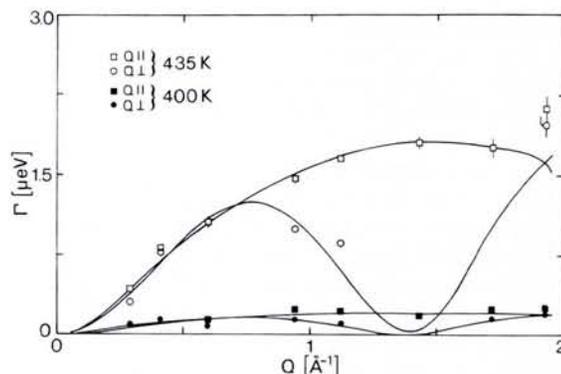
repeated trapping and release between the different layers, and a major part of hydrogen transport occurs along the empty layers. Diffusion perpendicular to the sheet is determined solely by the changeover processes between the different layers, but since the escape rate is much lower than the jump frequency, it is governed by the former.

Muon tracer studies
1. Experimental results

A positive muon in metals behaves like a light hydrogen isotope so it can be used as a radioactive tracer to determine the location of hydrogen atoms and hydrogen diffusion at higher hydrogen concentrations than experiments using hydrogen. With regard to diffusion, two aspects must be emphasized: a) At hydrogen concentrations above the percolation limit, the diffusion of the intrinsically fast-moving muon, captured in a cage of slow-moving hydrogen atoms, mirrors the diffusion of the sur-

Fig. 4 — Temperature dependence of the μ^+ depolarization rate in (nearly) stoichiometric VH$_{0.50}$. The low temperature plateaus are the static muon spin depolarization rates σ_o.

roundings, as has been shown for several metal/hydride systems.

b) In (nearly) stoichiometric hydrides where (nearly) all the regular hydrogen interstitial sites are occupied, an additional implanted muon is thermalized on one of the antistructural interstitial sites with the lowest energy, e.g., octahedral sites in TiH$_{2-x}$ (hydrogen is located on tetrahedral sites). For entropy reasons, a fraction of the hydrogen atoms also occupy these "forbidden" sites. Although very small in most cases, this fraction is of central importance for hydrogen diffusion, since in stoichiometric hydrides, the usually substantial diffusion on the hydrogen interstitial sublattice is ineffective owing to the lack of vacancies.

The minute but diffusionally active fraction is probed in μ^+ tracer studies, e.g., our investigation of the hydrogen diffusion mechanism in the ordered hydride β-VH$_{0.50}$ at low temperatures. Fig. 4 shows the temperature dependence of the depolarization rates σ of β-VH$_{0.50}$ measured using μSR. The muon behaviour is interpreted qualitatively as follows: below 80 K, the static depolarization rate σ_o, i.e. the plateau of the muon spin depolarization rate at low temperature, is large indicating that μ^+ is self-trapped on one of the available sites — in most cases antistructural sites in the empty layers since the sites in the larger regular H sublattice are blocked by hydrogen atoms. The drop of the relaxation rate around 100 K is due to intrinsic μ^+ diffusion in the empty layers. At about 180 K, muon diffusion is sufficiently rapid to allow a muon to find and be captured by a vacancy (a Type 1 trap) in the H sublattice within the muon's lifetime. The capture rate increases when hydrogen atoms start to occupy antistructural sites at 250 K, thus creating more and more vacancies in the regular sublattice. These new vacancies are termed dynamic traps (Type 2 traps) since they bear a close connection to the hydrogen dynamics.
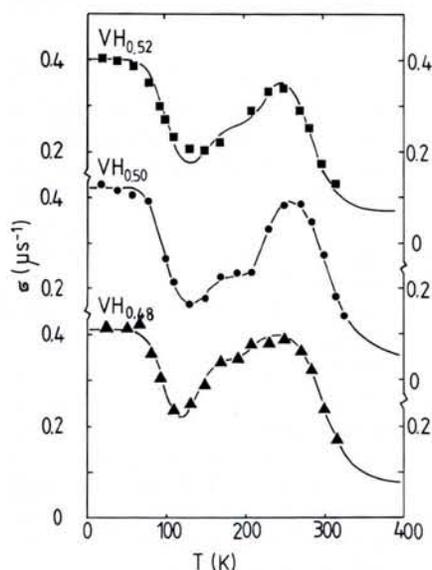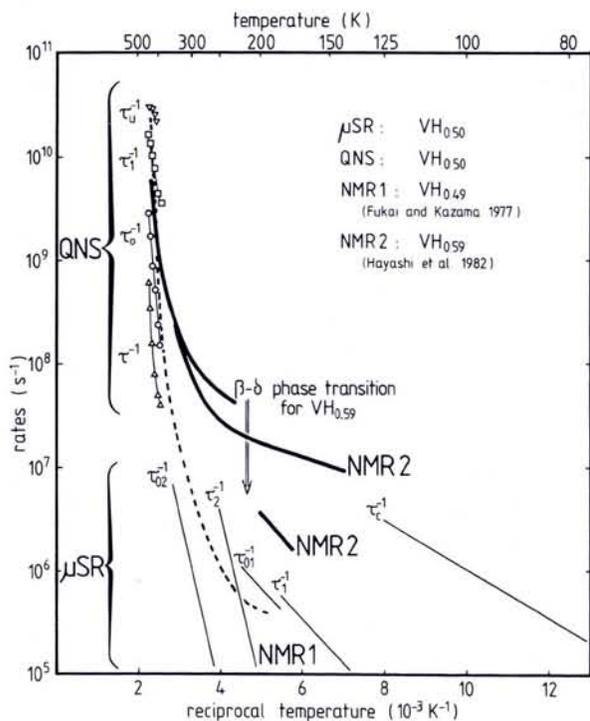
unique at low temperatures when the structure is well ordered.

NMR

We would like to emphasize that both QNS and μSR demonstrate directly that the hydrogen diffusion mechanism is complex and composed of several elementary jump rates, whereas NMR on stoichiometric $VH_{0.50}$ concludes this only indirectly from the observation of a curved Arrhenius plot. NMR on superstoichiometric $VH_{0.59}$ in fact indicates the presence of two different hydrogen populations (on structural and on antistructural octahedral sites), but that the second component below about 220 K is simply due to segregation of the β-phase (a two-phase sample). Thus, while NMR data for polycrystalline powders can only deliver global information about the hydrogen jump processes, it is very pleasing to see that they agree with the average of the QNS jump rates in the high temperature regime of Fig. 5, and with the average of the μSR jump rates in the low temperature regime. NMR provides a link between QNS and μSR, which essentially yield the same information about the hydrogen diffusion mechanism in $VH_{0.50}$, but in non-overlapping regimes because of different time windows.

Hydrogen Site Determination [8]

Several large Japanese companies are close to commercializing nickel/metal hydride rechargeable batteries. These batteries resemble Ni/Cd batte-
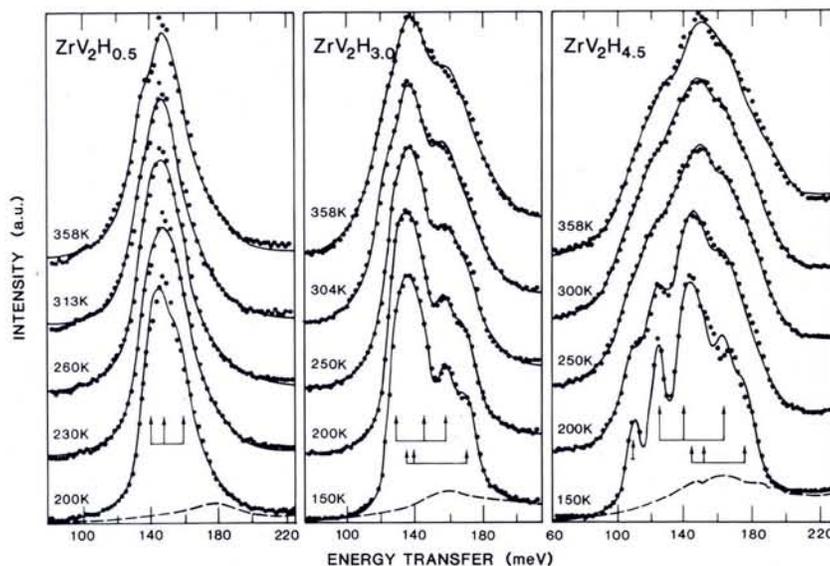
Eventually, above 300 K, the hydrogen atoms become sufficiently mobile and owing to fluctuations in the occupancy of the regular H sublattice, the muon can no longer be trapped but exhibits long-range diffusion: the vanishing depolarization rate indicates motional narrowing of the μ⁺ Larmor frequency distribution at temperatures above 300 K.

2. Analysis

Quantitatively, our μSR data were evaluated in terms of a three-state trapping model which considers repeated capture and release processes at both kinds of traps. We concluded that the correlation rate for μ⁺ diffusion in the empty planes, as well as the escape rate from the static traps, are intrinsic muon properties, connected, e.g., to the zero-point energy of the muon in its potential well. On the other hand, release from dynamic traps is closely related to the hydrogen dynamics: presumably a muon is only trapped in a fully intact next-nearest hydrogen surrounding, but is released even if only one of the neighbouring interstitial H atoms jumps away. This is in accordance with the observations that the μ⁺ activation energy for this jump process: a) corresponds exactly to the hydrogen activation energy, as measured by both QNS and NMR (see Fig. 5); and b) depends upon the hydrogen isotope. Thus, in this particular system (β-$VH_{0.50}$), the muon probes directly the hydrogen dynamics (equivalent to the dynamic traps).

It we compare, e.g., the correlation times and the lifetime in the free state τ_1 at 200 K and 100 K we note that, for $VH_{0.50}$, the muon performs about 17 jumps at 200 K and about 170 jumps at 100 K in the empty plane before it is captured in the H sublattice. The propagation path, which is "only" preferential in the temperature range of the QNS measurement close to the order-disorder transition, is therefore more or less

ries, but the negative CdOOH electrode has been replaced by a hydrogen electrode (the economic advantage is a higher charge capacity, the environmental advantage a Cd-free battery).

Neutron vibrational spectroscopy

One of the hydrogen storage materials which is used is $ZrV_{2-x}Ni_x$, where Ni as an indispensable catalyst replaces part of V in the parent cubic Laves phase ZrV_2. All interstitial sites in ZrV_2 are tetrahedral sites, but there are three kinds: Zr_2V_2, ZrV_3 and V_4 sites. A fundamental question concerns the location of the hydrogen in the storage material. Literature reports were contradictory before we started our combined neutron vibrational spectroscopy and muon spin rotation investigation.

The neutron results for three selected H concentrations show that the neutron vibrational spectrum for $ZrV_2H_{0.5}$, consisting of a comparatively narrow maximum at 145 MeV with two district shoulders, does not change much with temperature. We attribute this to the presence of hydrogen on the (energetically most favourable) Zr_2V_2 site, which owing to its low point-symmetry, gives rise to three non-degenerate vibrational modes.

The spectrum for $ZrV_2H_{3.0}$ exhibits additional scattering intensity on the low energy side of the main maximum which we attribute to an additional occupation of ZrV_3 sites. For $ZrV_2H_{4.5}$ we detect additional scattering on the high energy side of the main maximum which is assumed to be due to hydrogen atoms on V_4 sites. A quantitative comparison with the predictions of a simple dynamical model for the H vibrations confirmed this qualitative analysis.

µSR

A fortunate feature of the ZrVNi system in a µSR investigation is that the V nuclei possess a large nuclear magnetic moment and the Zr nuclei essentially none. The three types of sites mentioned above are therefore magnetically quite different, and easily distinguished using the second moment of the local magnetic field distribution, mirrored in the low temperature static muon spin depolarization rate σ_o (frozen-in muon).

In order to scan the available hydrogen sites with the positive muon, we charged ZrV_2 with hydrogen. At *low temperatures*, the H atoms occupy the lowest energy sites: the implanted muon will initially occupy one of the available sites at random. The low temperature plateau of the measured depolarization rate, *i.e.* the static muon spin

depolarization rate σ_o, increased with increasing H content so we conclude that more and more of the sites with the lowest σ, namely the Zr_2V_2 sites, become inaccessible to the muon. These are obviously the lowest energy sites. In $ZrV_2H_{3.25}H_{3.6}$, the measured values of the depolarization rate are close to the theoretical value for the ZrV_3 site, *i.e.*, at this H concentration the 12 Zr_2V_2 sites per formula unit are essentially blocked. This is a multiple site blocking, since an H atom blocks besides its own site about three other Zr_2V_2 sites, and resembles the situation in binary bcc metal hydrides, where blocking extending into the third coordination sphere has been observed.

Eventually, at the highest H concentrations ($ZrV_2H_{4.0}$ and $ZrV_2H_{4.8}$), the experimental depolarization rates are greater than theoretical values for the ZrV_3 sites: the majority of the ZrV_3 sites seems to be blocked and a large fraction of the muons is initially thermalized at a third type of site with a large σ, *i.e.*, a site surrounded by more than three vanadium atoms. This is the V_4 site.

Now consider the σ plateau at *intermediate temperatures*. At around 60 K, the thermal energy is apparently sufficient to release those muons which were initially thermalized at energetically unfavourable sites. They perform some diffusional jumps and very quickly find a vacancy in the sublattice of the energetically lower sites. The muons are trapped and — between 90 and 160 K — do not escape from these sites during their lifetime. Thus, in $ZrV_2H_{3.25}$, $ZrV_2H_{3.60}$ and $ZrV_2H_{4.0}$ the muons find empty Zr_2V_2 sites, whereas at the highest H concentration the number of vacancies in the Zr_2V_2 sublattice is obviously too small and the muons have to be content with ZrV_3 sites. ·

Conclusions

There exists an increasing number of cases where either neutron vibrational spectroscopy or muon spin resonance was used to determine hydrogen sites in metal alloys, but to our knowledge, the only example of where both neutrons and muons have been applied as microscopic probes of local atomic topology is the ZrV_2/H system.

For disordered metal/hydrogen systems, both approaches offer advantages over the standard diffraction technique owing to the lack of translational symmetry. We anticipate that the future will bring many more interesting and informative investigations using neutrons and muons. They are promising and prospering tools, not only in the vast field of disordered materials (ranging from a simple random solid solution of hydrogen in metals to the almost total disorder of hydrogen in metallic glasses), but also in more general research on metal/hydrogen systems.

FURTHER READING

[1] Springer T. and Richter D., "Neutron Scattering", *Methods of Experimental Physics* **23B**, p. 131; Eds. D.L. Price and K. Sköld (Academic Press, London) 1987.
[2] Richter D., "Neutron Scattering and Muon Spin Rotation", *Springer Tracts in Modern Physics* **101** (Springer, Berlin) 1983.
[3] Kondo J. in "Fermi Surface Effects", Eds. J. Kondo and A. Yoshimo, *Springer Series in Solid State Sciences* **77** (1988).
[4] Kehr K.W. *et al.*, *Phys. Rev. B* **26** (1982) 567; Hartman O. *et al.*, *Phys. Rev. B* **37** (1988) 4425.
[5] Steinbinder D. *et al.*, *Europhys. Lett.* **6** (1988) 535.
[6] Richter D. *et al.*, *Z. Phys. Chem. NF* **164** (1989) 907.
[7] Hempelmann R. *et al.*, *J. Less-Common Metals* (1991) in print.
[8] Hempelmann R. *et al.*, *J. Phys. Chem.* **90** (1989) 1935.